Since January 2020 Elsevier has created a COVID-19 resource centre with free information in English and Mandarin on the novel coronavirus COVID-19. The COVID-19 resource centre is hosted on Elsevier Connect, the company's public news and information website.

Bioorganic & Medicinal Chemistry 23 (2015) 5345–5351

Contents lists available at ScienceDirect

Bioorganic & Medicinal Chemistry

journal homepage: www.elsevier.com/locate/bmc

Carbon nanotubes supported tyrosinase in the synthesis of lipophilic hydroxytyrosol and dihydrocaffeoyl catechols with antiviral activity against DNA and RNA viruses

Giorgia Botta [a], Bruno Mattia Bizzarri [a], Adriana Garozzo [b], Rossella Timpanaro [b], Benedetta Bisignano [b], Donatella Amatore [c,d], Anna Teresa Palamara [c,d], Lucia Nencioni [c,*], Raffaele Saladino [a,*]

[a] Department of Ecology and Biology, University of Tuscia, Largo dell'Università, 01100 Viterbo (VT), Italy
[b] Department of Biomedical and Biotechnological Sciences, Microbiological Section, University of Catania (CT), Via Androne, 81 95124 Catania, Italy
[c] Department of Public Health and Infectious Diseases, 'Sapienza' University, 00185 Rome, Italy
[d] IRCCS San Raffaele Pisana, Telematic University, 00166 Rome, Italy

ARTICLE INFO

Article history:
Received 28 May 2015
Revised 24 July 2015
Accepted 27 July 2015
Available online 30 July 2015

Keywords:
Antiviral activity
Catechols
Hydroxytyrosol derivatives
Dihydrocaffeoyl derivatives
DNA and RNA viruses

ABSTRACT

Hydroxytyrosol and dihydrocaffeoyl catechols with lipophilic properties have been synthesized in high yield using tyrosinase immobilized on multi-walled carbon nanotubes by the Layer-by-Layer technique. All synthesized catechols were evaluated against a large panel of DNA and RNA viruses, including Poliovirus type 1, Echovirus type 9, Herpes simplex virus type 1 (HSV-1), Herpes simplex virus type 2 (HSV-2), Coxsackievirus type B3 (Cox B3), Adenovirus type 2 and type 5 and Cytomegalovirus (CMV). A significant antiviral activity was observed in the inhibition of HSV-1, HSV-2, Cox B3 and CMV. The mechanism of action of the most active dihydrocaffeoyl derivative was investigated against a model of HSV-1 infection.

1. Introduction

Catechol derivatives show different biological properties, including inhibition of hypoxia inducible factor-prolyl hydroxylase-2 (HPH) in the treatment of colitis,[1] antiepileptogenic,[2] pulmonary fibrosis,[3] anticancer,[4–6] antimicrobial,[7] and anti-Parkinson activities.[8] Moreover, they are active against viruses, as in the case of rhinovirus,[9] HIV-1 integrase,[10,11] HIV-1 reverse transcriptase,[12] and coronavirus.[13] The biological activity of catechols is associated to their antioxidant property, that is the capacity of transferring single-electron and/or hydrogen-atom to reactive free radicals,[14–16] as well as, to binding pro-oxidant metal ions.[17] The antioxidant activity can be oriented toward specific cellular compartments by controlling the chemical and physical properties of the substituents on the aromatic ring.[18] For example, the limited accessibility of highly hydrophilic catechols to specific intracellular targets has been improved by the synthesis of lipophilic derivatives possessing long carbon alkyl side chains.[19–21] In the case of bioactive hydroxytyrosol and dihydrocaffeic acid derivatives,[22,23] which are characterized by the concomitant presence of alcoholic and *ortho*-diphenol groups,[24,25] the side-chain functionalization requires expensive and tedious protection/deprotection sequences. As an alternative, we described the synthesis of lipophilic catechols by selective oxidation of side-chain functionalized phenol derivatives, using tyrosinase supported on Eupergit C250L resin (Tyr/ECM), by sequential deposition of alternatively charged poly(allylamine hydrochloride) (PAH) and polystyrene sulfonate (PSS).[26] Tyrosinase is a copper enzyme which catalyzes the hydroxylation of monophenols to *ortho*-diphenols and *ortho*-quinones using dioxygen (O_2) as primary oxidant.[27] In this latter case, dihydrocaffeoyl catechols showed antiviral activity against Influenza A virus, an infection that continue to represent a severe threat wordwide.[28] Derivatives characterized by antioxidant activity and longer carbon alkyl side-chains were more effective, suggesting the possibility of novel inhibition mechanisms based on both redox and lipophilic properties.[26] These data were in accordance with previous findings about the activity of lipophilic glutathione (GSH) derivatives, which were able to enter into the cell more easily than GSH, thus inhibiting the replication of DNA and RNA viruses.[29] The efficacy of tyrosinase in the synthesis of simple catechol derivatives was successively increased by immobilization of the enzyme on multi-walled carbonanotubes (MWCNTs), using the Layer-by-Layer (LbL) procedure.[30] The LbL procedure is based on

* Corresponding authors.
E-mail address: saladino@unitus.it (R. Saladino).

http://dx.doi.org/10.1016/j.bmc.2015.07.061
0968-0896/

the consecutive deposition of alternatively charged polyelectrolytes onto the active species, able to protect proteins from high-molecular-weight denaturing agents.[31] MWCNTs are characterized by high surface area for enzyme loading, as well as biocompatibility, and favorable electrochemical and mechanical properties.[32,33] The best catalyst (indicated in the follow as MWCNT/Tyr) was obtained by co-immobilization of Tyr and Bovine Serum Albumin (BSA) on oxidized MWCNTs, in the presence of polydiallyldimethyl ammonium chloride (PDDA).[30] Here we report the use of MWCNT/Tyr for the improved synthesis of lipophilic hydroxytyrosol and dihydrocaffeoyl catechols, and their antiviral activity against a large panel of DNA and RNA viruses, including Poliovirus type 1, Echovirus type 9, Herpes simplex virus type 1 (HSV-1) and type 2 (HSV-2), Coxsackie virus type B3 (Cox B3), Adenovirus type 2 and type 5, and Cytomegalovirus (CMV). Some of these compounds were endowed with antiviral activity at sub-toxic concentrations. The mechanism of action of the most active dihydrocaffeoyl derivative was investigated in detail against a model of HSV-1 infection.

2. Results and discussion

The MWCNT/Tyr was prepared as previously reported.[30] Briefly, mushroom Tyr from *Agaricus bisporus* and BSA (BSA/Tyr ratio 3:1) were immobilized on oxidized MWCNTs,[34] by deposition of a layer of PDDA (MWCNTs-PDDA/Tyr ratio of 5:1) in sodium phosphate buffer (PBS; 0.1 M, pH 7) at room temperature (Fig. 1, step A). The excess PDDA was removed by centrifugation/re-dispersion cycles since residual PDDA in the solution can precipitate upon mixing with enzyme. The concentration of adsorbed PDDA was evaluated by UV–vis analysis (at 595 nm) of the supernatant after treatment with Comassie Brillant Blue (CBB) (experimental details and the calibration curve for PDDA are in Supplementary information, SI # 1, Table A, Fig. 1).[35] The amount of PDDA adsorbed per mg of starting material was found to be 0.58 ± 0.01 mg. This amount is similar to the 'just enough' amount of PDDA (0.48 mg) required to cover all the surface of MWCNTs (100% covering efficacy), as previously reported.[36]

The presence of cationic PDDA facilitates the loading of Tyr, that is negatively charged at the operative pH 7.0 (isoelectric point of Tyr 4.7–5.0).[37] Bovine Serum Albumin (BSA), an inert enzyme characterized by an isoelectric point close to Tyr, was used during the co-immobilization procedure to reduce the surface area available to the enzyme, avoiding undesired conformational changes due to enzyme strives for the greatest surface coverage.[38] Glutaraldehyde (GA) was then added to increase the reticulation grade and stability of the catalyst (Fig. 1, step B).[39] Crosslinking with glutaraldehyde is a widely applied procedure for the immobilization/reticulation of enzymes on different kind of support.[40] In accordance with data reported in the literature,[41] the effectiveness of the crosslinking procedure was confirmed by FT-IR analysis, observing the appearance of a new absorption band in the range of 1700–2100 cm^{-1} attributable to the formation of Schiff bases (representative FT-IR spectra of MWCNT/Tyr with or without GA are in Supplementary information, SI # 2, Figs. 2 and 3). The activity of native Tyr (81.2 U/mg) was determined by the dopachrome assay following the oxidation of L-tyrosine at 475 nm (the enzyme unit is defined as the increase in absorbance of 10^{-3} unit/min at 25 °C in 0.1 M phosphate buffer, pH 7.0).[42] The activity of MWCNT/Tyr (80.5 U/mg), and the value of activity parameters, namely immobilization yield (68%), and activity yield (48.5%), were in accordance with our previous data (for the definition of these parameters see in the experimental part).[30] The Scanning Electron Microscopy (SEM) and Atomic Force Microscopy (AFM) of MWCNT/Tyr were in accordance with data previously reported, and confirmed the polyelectrolyte deposition and enzyme immobilization.[30] In particular, the AFM analysis clearly showed functionalized nanotubes characterized by a smooth surface probably due to the presence of BSA in the interstitial sites between Tyr molecules. The maximum height and width were higher than that observed for MWCNTs alone (experimental procedures, SEM analysis, and magnified details of the bi-dimensional high resolution AFM images of MWCNT/Ty and MWCNTs with the corresponding profiles, are in Supplementary information SI #3, Figs. 4 and 5).[30]

Kinetic parameters for native Tyr and MWCNT/Tyr were evaluated in CH_2Cl_2 and PBS, using tyrosol acetate **2a** as a selected substrate to be oxidized (see next). The initial reaction rates were measured at substrate concentrations ranging from 1.0 to 20 mM at 25 °C. Kinetic constants were evaluated by using different linear regression equations (Lineweaver–Burk, Hanes and Eadie–Hofstee). The kinetic parameters (K_m, V_{max}, and K_{cat}) for the native enzyme and MWCNT/Tyr are reported in Table 1. MWCNT/Tyr shows a performance about two times lower than the native enzyme, in agreement with the expected decrease of catalytic efficiency after immobilization. The catalytic efficacy of MWCNT/Tyr (defined as V_{max}/K_m) was found to be 81.7 10^{-4} (as the average value of the three tests). The ester derivatives of commercially available 3(4-hydroxyphenyl)propanoic acid **1** and tyrosol **2** (4-hydroxyphenylethyl alcohol) were used as substrates. In particular, the ester derivatives **1a–d** (Scheme 1) were prepared by reaction of **1** with an excess of the appropriate alcohol in the presence of trimethylchlorosilane (TMCS) at 25 °C (experimental details are in Supporting SI #4).[43]

The esterification of **2** to yield compounds **2a–d** (Scheme 2) was carried-out using lipase from *Candida antarctica* to avoid the possible formation of mixture of esters, due to competition between alcoholic and phenol groups (Supporting SI #5).[44] The oxidation of compounds **1** and **1a–d** (0.05 mmol) was performed with MWCNT/Tyr (240 U) in CH_2Cl_2/buffer (Na phosphate 0.1 M pH 7, CH_2Cl_2/buffer ratio 1.0:0.1) at 25 °C under O_2 atmosphere for 24 h (Scheme 1, Table 2). The use of CH_2Cl_2 as reaction solvent was necessary to increase the solubility of hydrophobic substrates,

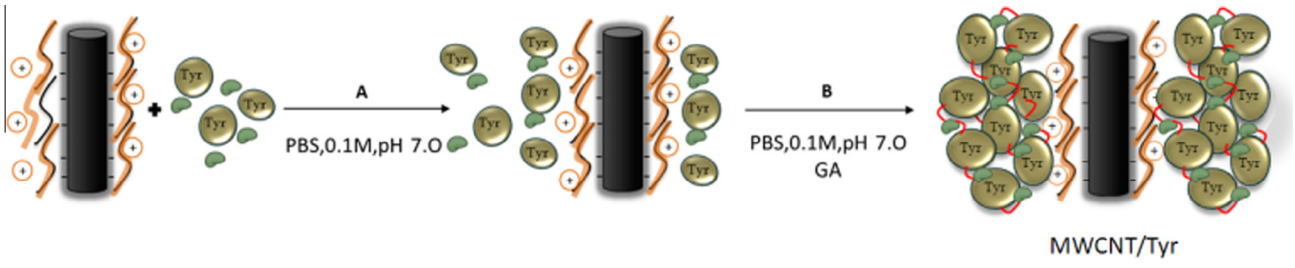

Figure 1. Preparation of MWCNT/Tyr. Step A: coating of Tyr and BSA on functionalized PDDA/MWCNTs. Step B: cross-linking with GA.

Table 1
Kinetic parameters for native tyrosinase (Tyr) and catalyst MWCNT/Tyr[a]

Plot	K_m (mM)		$V_{max}\cdot10^4$ (ΔAbs·min^{-1}·μg enzyme^{-1})		K_{cat} (min^{-1})	
	Tyr	MWCNT/Tyr	Tyr	MWCNT/Tyr	Tyr	MWCNT/Tyr
Lineweaver-Burk	0.13	0.10	30	6	909	181
Hanes	0.11	0.15	27	14	818	424
Eadie-Hofstee	0.11	0.13	26	12	788	364

[a] K_{cat} is defined as v_{max} (Δabsorbance per minute)/[Tyr] (micromoles per milliliter). All experiments were conducted in triplicate using free and immobilized tyrosinase. Average errors in kinetic parameters were 2–4% for K_m and 1–3% for V_{max}.

in accordance with improved stability and selectivity (with limited formation of *ortho*-benzoquinones and polymeric side-products) reported for Tyr in organic solvents.[45]

The oxidation of **1** and **1a** (as selected samples) was also performed using previously reported Tyr/ECM as reference, in which Tyr is covalently immobilized on micro-spheres of the synthetic resin Eupergit C250L (methacrylamide, *N*,*N*′-methylen-bis-acrylamide polymer).[26] MWCNT/Tyr selectively afforded catechol derivatives **3** and **3a**–**d** in quantitative conversion of substrate and yield of product (Table 2). In these reactions, MWCNT/Tyr showed a reactivity similar to Tyr, and higher than Tyr/ECM (Table 2, entry 3 versus entries 1 and 2, and entry 6 versus entries 4 and 5). In this latter case 600 U were required to obtain the quantitative yield of products (Table 1, entries 2, 5 and 10).

These data further confirm the benign role of MWCNT as nano-sized supports for the immobilization of Tyr in synthetic applications. In a similar way, the oxidation of tyrosol esters **2a**–**d** afforded the corresponding lipophilic catechols **4a**–**d** (Scheme 2) in quantitative conversion of substrate and yield of product (Table 2, entries 10–14). Again, MWCNT/Tyr performed better than Tyr/ECM (Table 2, entry 11 vs entry 10). Recycling experiments proceeded with success in the oxidation of compound **1** under similar experimental conditions. After the first oxidation, MWCNT/Tyr was recovered by centrifugation, washed, and reused with fresh substrate. As shown in Table 3, MWCNT/Tyr was used for at least six cycles with only a slight decrease of efficiency to give **3** (Table 3, entry 1 vs entry 6). Note that MWCNT/Tyr was more stable than Tyr/ECM, for which a significant decrease in the activity was observed (ca. 37%; Table 3, entry 1 vs entry 6).

3. Antiviral activity

The development of antiviral agents has progressed rapidly over the last decades. The drugs approved for use generally inhibit specific steps of viral replication usually by targeting viral proteins with an enzymatic function. Unfortunately, a large majority of the available antiviral drugs are limited in their efficacy by systemic toxicity and drug resistance.[46] Many different circumstances favor the selection of drug resistant strains, for example, high viral loads, intrinsic mutation rates, and prolonged exposure to the drug. For this reason, natural or de-novo designed molecules able to inhibit the replication of DNA or RNA viruses with different mechanisms have been synthesized.[47–52] The antiviral activity of lipophilic catechol derivatives **3**, **3a**–**d**, and **4a**–**d** was evaluated against several DNA and RNA viruses (Polio 1, Echo 9, HSV-1, HSV-2, Cox B3, Adeno 2, Adeno 5 and CMV). Cell monolayers were infected at multiplicity of infection (MOI) 0.1 and treated with different concentrations (ranging from 25 to 200 μg/mL) of each compound. The values of CD_{50} (concentration which inhibited cells growth by 50% when compared with control culture) and ID_{50} (concentration which inhibited virus plaque formation and virus-induced cytopathogenicity by 50%) of catechol derivatives are shown in Tables 4 and 5, respectively.

Derivatives **3b**, **3d**, **4a** and **4b** were characterized by selective antiviral activity. In particular, compounds **3b** and **4a** demonstrated the highest level of activity against HSV-1 (DNA virus), with ID_{50} values of 15 and 20 μg/mL, respectively. Moreover, the same compounds showed slight activity against HSV-2 (60 and 40 μg/mL, respectively) and Cox B3 (RNA virus; 20 and 50 μg/mL, respectively). With regard to **4b**, a modest activity against HSV-1 was observed, probably due to toxic effect on cell monolayer, as suggested by the low value of CD_{50} (40 μg/mL). Finally, **3b** and **3d** were effective against CMV (DNA virus), **3d** being the most active compound with an ID_{50} value of 25 μg/mL. Since **3b** was effective against several RNA or DNA viruses, especially in the case of herpetic viruses (HSV-1, HSV-2 and CMV), its mechanism of action was investigated in more detail using a model of HSV-1 infection. In particular, compound **3b** was added at different times on VERO cells infected with 0.1 MOI of HSV-1, to determine the inhibition of the virus yield during specific periods in the virus life-cycle. The results clearly demonstrate that **3b** interferes with an early step of the viral replicative cycle. Indeed, the viral replication was blocked during the first hour of infection. Otherwise, no reduction was observed when **3b** was added after 2 h. Moreover, a slight reduction of virus yield was observed during the adsorption period (Fig. 2).

As **3b** exerted its activity through the inhibition of the early events in HSV-1 replication, we set up some experiments in order to deepen its mechanism of action. First, the effect of the compound was studied during the viral adsorption period by means of the infective center assay. Results obtained from this experiment demonstrated that **3b** did not significantly inhibit adsorption of HSV-1 at concentrations higher than 5 times the ID_{50} (Fig. 3). Furthermore, it was important to establish if any virucidal effect

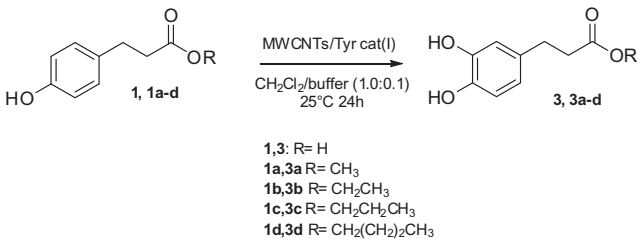

Scheme 1. Oxidation of compounds **1** and **1a**–**d** with MWCNT/Tyr.

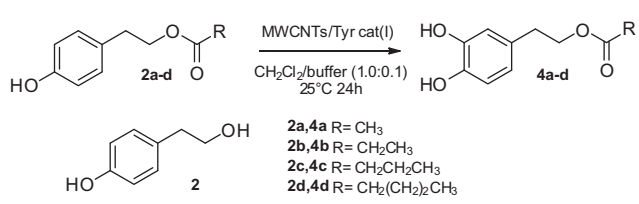

Scheme 2. Oxidation of compounds **2a**–**d** with MWCNT/Tyr.

Table 2
Synthesis of hydroxytyrosol and dihydrocaffeoyl catechol derivatives **3**, **3a–d** and **4a–d**[a]

Entry	Substrate	Catalyst	Product	Conversion (%)	Yield (%)
1	**1**	Tyr	**3**	98	98
2	**1**	Tyr/ECM	**3**	45	44[b]
3	**1**	MWCNT/Tyr	**3**	98	98
4	**1a**	Tyr	**3a**	98	98
5	**1a**	Tyr/ECM	**3a**	47	46[b]
6	**1a**	MWCNT/Tyr	**3a**	98	98
7	**1b**	MWCNT/Tyr	**3b**	98	98
8	**1c**	MWCNT/Tyr	**3c**	98	98
9	**1d**	MWCNT/Tyr	**3d**	98	98
10	**2a**	Tyr/ECM	**4a**	53	51[b]
11	**2a**	MWCNT/Tyr	**4a**	98	98
12	**2b**	MWCNT/Tyr	**4b**	98	98
13	**2c**	MWCNT/Tyr	**4c**	98	98
14	**2d**	MWCNT/Tyr	**4d**	98	98

[a] The oxidation was performed on 0.05 mmol of substrate with the appropriate catalyst (240 units) in CH_2Cl_2/buffer (Na phosphate 0.1 M pH 7, CH_2Cl_2/buffer ratio 1.0:0.1) at 25 °C under O_2 atmosphere for 24 h.
[b] In this case an higher amount of immobilized enzyme (600 units) was required to obtain a quantitative yield of desired product.

Table 3
Reusability of MWCNT/Tyr and Tyr/ECM in the oxidation of 1[a,b]

Entry	Run	Tyr/ECM (yield%)	MWCTN/Tyr (yield%)
1	1	46	98
2	2	46	98
3	3	41	98
4	4	36	97
5	5	32	95
6	6	29	91

[a] Reusability is expressed as the yield in% of catechol **3** obtained by oxidation of **1** with Tyr/ECM-LbL and MWCTN/Tyr.
[b] The oxidation of **1** (0.05 mmol) was performed in the presence of the appropriate catalyst (240 units) in CH_2Cl_2/buffer (Na phosphate 0.1 M pH 7, CH_2Cl_2/buffer ratio 1.0:0.1) at 25 °C under O_2 atmosphere for 24 h.

or protective actions for Vero cells was produced. Our results demonstrated that **3b** was not virucidal for HSV-1 and did not exerted any protective action for the cells, thus suggesting that the reduction in the virus yield, immediately after the adsorption period, could be related to the interference of the compound with penetration, un-coating and/or another early step of HSV-1 replication.

Table 4
Antiviral activity of cathecol derivatives **3**, **3a–d** and **4a–d** against different DNA and RNA viruses

Compound	ID_{50}[a,b] (μg/mL)							
	Polio 1	CoxB3	ECHO9	HSV-1	HSV-2	Adeno 2	Adeno 5	CMV
3	>200	>200	>200	>200	ND	>200	>200	>200
3a	>100	>100	>100	>100	>100	>100	>100	100
3b	>75	20	>75	15	60	>40	>40	40
3c	>200	>200	>200	>200	ND	>200	>200	ND
3d	>200	100	>200	>200	>200	>200	>200	25
4°	>100	50	>100	20	40	>50	>50	>50
4b	>40	>40	>40	20	40	>40	>40	>40
4c	>100	>100	>100	>100	100	>100	>100	>100
4d	>25	>25	>25	25	ND	>25	>25	>25

[a] Values are mean ± 0·5 SD (maximal SD estimated) for three separate assays.
[b] ID_{50}, concentration which inhibited virus plaque formation and virus-induced cytopathogenicity by 50%.

Table 5
Cytotoxicity of cathecol derivatives **3**, **3a–d** and **4a–d**

Compound	CD_{50}[a,b] (μg/mL)		
	VERO	HEp2	HFF1
3	>200	>200	>200
3a	100	100	100
3b	75	40	40
3c	>200	>200	ND
3d	200	200	100
4a	100	50	50
4b	40	40	40
4c	100	100	100
4d	25	25	25

[a] Values are mean ± 0·5 SD (maximal SD estimated) for three separate assays.
[b] CD_{50}, concentration which inhibited cells growth by 50% when compared with control culture.

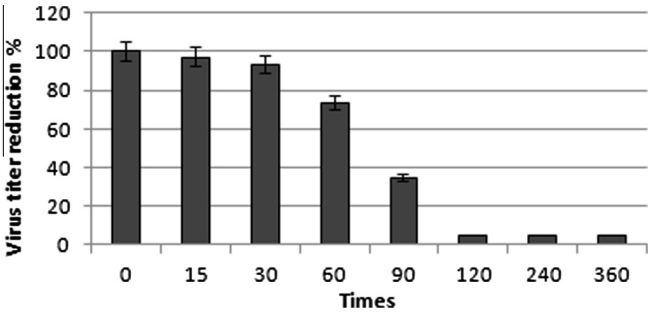

Figure 2. Effect of addition of compound **3b** (5 × ID_{50}) at various times during the replicative cycle of HSV-1. Time 0 = post 2 h adsorption period at 4 °C. The concentrations used are ratios with respect to the ID_{50} (e.g., 5× the ID_{50} is 5 times the ID_{50} of the compound). Each value represents the mean ± SEM of three separate assays.

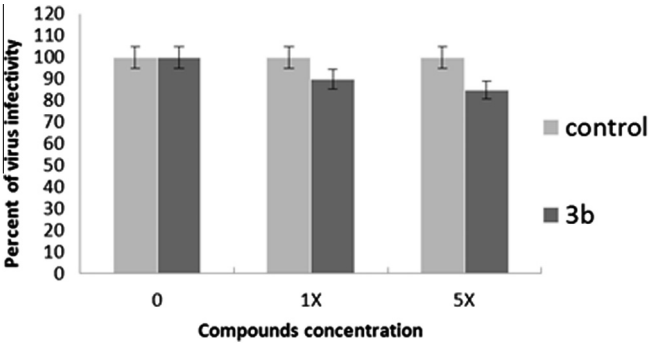

Figure 3. Effect of compound **3b** (1×, 5× ID_{50}) on the adsorption of HSV-1. Infective center assay data were plotted as percentage of virus infectivity relative to the no-drug control. The concentrations used are ratios with respect to the ID_{50}.

4. Conclusions

MWCNTs/Tyr was an efficient catalyst for the synthesis of tyrosol and dihydrocaffeoyl catechols by oxidation of phenol ester derivatives under mild experimental conditions, in quantitative conversion of substrate and yield. The activity of MWCNT/Tyr was comparable to native Tyr and greater than previously reported Tyr/E-250 catalyst, confirming the benign role of carbon nanotubes in the enzyme immobilization process. MWCNT/Tyr was a stable catalyst for at least six recycle experiments. Among lipophilic catechols, compounds **3b**, **3d**, **4a** and **4b** were active against HSV-1, HSV-2, Cox B3 and CMV. In a previous study, compounds **4a** and **4b** were also active against influenza A/PR8/H1N1 virus, showing

the highest antioxidant activity as measured by the 2,2-diphenyilpicrylhydrazyl (DPPH) radical scavenging assay.[26] In the case of the inhibition of HSV-1 and HSV-2 viruses, the highest antiviral activity prevailed in derivatives characterized by a low/medium long alkyl side-chain. The mechanism of action of compound **3b** was studied in detail using a model of HSV-1 infection. Data showed that the inhibition of virus replication was effective in earlier stages of the replication cycle, probably related to penetration, un-coating and/or another early step of HSV-1 replication.

5. Experimental

5.1. Materials

Mushroom tyrosinase from Agaricus bisporus (Tyr), multi-walled carbon nanotubes (MWCNTs), L-tyrosine, bovine serum albumin (BSA), glutaraldehyde (GA), polydiallyldimethylammonium chloride (PDDA), sodium sulfate anhydrous (Na_2SO_4), 3(4-hydroxyphenyl)propanoic acid **1**,,tyrosol (4-hydroxy phenyl ethyl alcohol) **2**, alcohols and organic solvents were purchased from Sigma–Aldrich. All spectrophotometric measurements were made with a Varian Cary50 UV–vis spectrophotometer equipped with a Peltier thermostatted single cell holder. FT-IR measurements were performed using a Perkin Elmer FT-IR spectrometer in KBr. All samples were dried before the analysis. ^{1}H NMR and ^{13}C NMR spectra were recorded on a Bruker (400 MHz) spectrometer. Mass spectra were recorded on a VG 70/250S spectrometer with an electron beam of 70 eV. Dichloromethane (CH_2Cl_2) was dried on anhydrous sodium sulfate prior to use. All experiments were done in triplicate using native and immobilized tyrosinase in dichloromethane/buffer system and in H_2O medium. Sodium phosphate [(PBS) 0.1 M, pH 7.0] was used as the buffer solution.

5.2. Preparation of catalyst MWCNT/Tyr

MWCNT/Tyr was prepared as previously reported.[30] Briefly, PDDA coated MWCNTs in PBS were treated with a mixture of Tyr (0.2 mg) and BSA (0.6 mg) for 30 min. Glutaraldehyde (GA, 2.5%) was added to reach a final volume of 800 μL and the mixture was shaken at 25 °C for 30 min and at 4 °C overnight. The excess enzyme and GA were removed by centrifugation (6000 rpm × 20 min) and the surnatant was used for the calculation of activity parameters. The catalyst was finally treated with 1.5 mL TRIS–HCl 0.1 M pH 7.2 by shaking for 1h at 4 °C and centrifuged. MWCNT/Tyr was washed several times with PBS in order to ensure the complete removal of unbounded Tyr (as evaluated by the Bradford method).

5.3. Activity data

The activity of native and immobilized Tyr was determined by measuring the oxidation of L-tyrosine. The reaction was started by adding L-tyrosine to the solution of Tyr or MWCNT/Tyr in PBS under magnetic stirring. The initial rates were measured as linear increase in optical density at 475 nm, due to dopachrome formation. One unit of enzyme activity was defined as the increase in absorbance of 0.001 per minute at pH 7, 25 °C in a 3.0 mL reaction cuvette containing 0.83 mM of L-tyrosine and 67 mM of PBS pH 7.0. The activity was expressed as activity unit per milligram of support:

$$\text{Activity (U/mg)} = \text{Ux/Wsupport}$$

where: Ux is the activity of the immobilized enzyme assayed by dopachrome method. The activity yield represents the % of the ratio of activity of the immobilized enzyme to the total units of native enzyme used:

$$\text{Activity yield } (\%) = [\text{Ux}/(\text{Ua} - \text{Ur})] \cdot 100$$

where: Ua is the total activity of enzyme (unit) added in the solution and Ur is the activity of the residual Tyr (unit) evaluated by dopachrome method in the washing solutions. The immobilization yield is defined as:

$$\text{Immobilization yield } (\%) = [(\text{Ua} - \text{Ur})/\text{Ua}] \cdot 100.$$

5.4. Determination of the kinetic constants

The catalytic properties of native and immobilized tyrosinase were determined in the organic solvent media by measuring initial rates of the reaction with the substrate at 25 °C. The reactions were carried out by using different concentrations of tyrosol acetate **2a**, ranging from 1 to 20 mM. The appropriate amount of **2a** was dissolved in DCM (2.5 mL) and free or immobilized tyrosinase in the optimum aqueous amount (275 μL of PBS) was added. The reaction mixture was stirred for 30 min. Sampling was performed every 6.0 min, the absorbance at 395 nm was measured and the sample returned to the flask as rapidly as possible. One unit of enzyme activity was defined as the increase in absorbance of 0.001 at 395 nm, 25 °C, CH_2Cl_2 and PBS 0.1 M, pH 7.0. K_m and V_{max} values were calculated by plotting data in Lineweaver-Burk, Hanes and Eadie–Hofstee.

5.5. Synthesis of catechol derivatives 3, 3a–d and 4a–d

MWCNT/Tyr (240 U) was added to a solution of the appropriate substrate (0.05 mmol) in CH_2Cl_2 (2.5 mL) in PBS (275 μL), and the mixture was stirred at 25 °C under O_2. After 24 h, the catalyst was recovered by centrifugation and the organic fraction was concentrated and treated with a solution of sodium dithionite in THF and H_2O [1:1 (v/v)]. The mixture was stirred at 25 °C for 5 min to allow the complete reduction of benzoquinones to catechols and extracted twice with ethyl acetate (EtOAc; 2.0 mL × 2). The collected organic extracts were dried over anhydrous sodium sulfate, filtered and concentrated under vacuum to yield catechol derivatives **3**, **3a–d** and **4a–d**. All experiments were conducted in triplicate. The structure of catechol derivatives was characterized without further purification by comparison with data previously reported in the literature.[26]

5.5.1. (3,4-Dihydroxyphenyl)propanoic acid (3)

Oil; ^{1}H NMR (400 MHz, $CDCl_3$): δH (ppm) = 2.64 (2H, m, CH_2), 2.81 (2H, m, CH_2), 6.76–6.94 (3H, m, Ph-H); ^{13}C NMR (50 MHz,$CDCl_3$): δC (ppm) = 30.44 (CH_2), 35.81 (CH_2),115.36 (2 × CH), 119.46 (CH), 132.33 (C), 145.10 (C), 145.93 (C), 174.98 (CO); MS (EI): *m*/*z* 398; elemental analysis: calcd C, 59.34; H, 5.53; O, 35.13, found C, 59.30; H, 5.53; O, 35.04.

5.5.2. 3-(3,4-Dihydroxyphenyl)propanoic acid methyl ester (3a)

Oil; ^{1}H NMR (400 MHz, $CDCl_3$): δH (ppm) = 2.56 (2H, m, CH_2), 3.57 (3H, s, OCH_3), 6.8–7.1 (3H, m, Ph-H); ^{13}C NMR (50 MHz, $CDCl_3$): δC (ppm) = 30.68 (CH_2), 35.68 (CH_2), 51.60 (CH_3), 115.90 (CH), 116.20 (CH), 120.30 (CH), 133.30 (C), 144.20 (C), 145.70 (C), 173.65 (CO); MS (EI): *m*/*z* 340; elemental analysis: calcd C, 61.22; H, 6.16; O, 32.62, found C, 61.20; H, 6.16; O, 32.68.

5.5.3. 3-(3,4-Dihydroxyphenyl)propanoic acid ethyl ester (3b)

Oil; ^{1}H NMR(400 MHz, $CDCl_3$) δH (ppm) = 1.18 (3H, m, CH_3), 2.48 (2H, m, CH_2), 2.72 (2H, m, CH_2), 4.05 (2H, m, OCH_2), 6.65–6.71 (3H, m, Ph-H); ^{13}C NMR (50 MHz, $CDCl_3$): δC (ppm) = 16.10 (CH_3), 36.07 (CH_2), 60.10 (CH_2), 117.00 (2 CH), 120.30 (CH), 133.30 (C), 144.20 (C), 145.70 (C), 172.10 (CO); MS (EI): *m*/*z* 354; elemental analysis: calcd C, 62.85; H, 6.71; O, 30.44, found C,62.81; H, 6.71; O, 30.37.

5.5.4. 3-(3,4-Dihydroxyphenyl)propanoic acid propyl ester (3c)

Oil; ^{1}H NMR(400 MHz, $CDCl_3$): δH (ppm) = 1.20–1.35 (5H, m, CH_2+CH_3), 2.55 (2H, m, CH_2), 2.82 (2H, m, CH_2), 4.15 (2H, m, OCH_2), 6.40–6.80 (3H, m, Ph-H); ^{13}C NMR (50 MHz, $CDCl_3$): δC (ppm) = 10.35 (CH_3), 22.03 (CH_2), 30.68 (CH_2), 35.95 (CH_2), 65.79 (CH_2), 115.90 (CH), 116.20 (CH), 120.30 (CH), 132.51 (C), 114.20(C), 145.60 (C), 172.15 (CO); MS (EI): *m*/*z* 368; elemental analysis: calcd C, 64.27; H, 7.19; O, 28.54, found C, 64.38; H, 7.18; O, 28.44.

5.5.5. 3-(3,4-Dihydroxyphenyl)propanoic acid butyl ester (3d)

Oil; ^{1}H NMR(400 MHz, $CDCl_3$): δH (ppm) = 0.90 (3H, m, CH_3), 1.20 (2H, m, CH_2), 2.50 (2H, m, CH_2), 2.80 (2H, m, CH_2), 3.50 (2H, m, CH_2), 4.10 (2H, m, OCH_2), 6.50–7.80 (3H, m, Ph-H); ^{13}C NMR (50 MHz, $CDCl_3$): δC (ppm) = 16.10 (CH_3), 19.13 (CH_2), 30.10 (2 CH_2), 36.34 (CH_2), 64.10 (CH_2), 115.45 (2 CH), 129.10 (CH), 129.50 (C), 137 (C), 143.10 (C), 173.20 (CO); MS (EI): *m*/*z* 382; elemental analysis: calcd C, 65.53; H, 7.61; O, 26.86, found C, 65.45; H, 7.61; O, 26.75.

5.5.6. Hydroxytyrosol acetate (4a)

Oil; ^{1}H NMR(400 MHz, $CDCl_3$): δH (ppm) = 2.13 (3H, s, CH_3), 2.75 (2H, m, OCH_2), 4.17 (2H, m, CH_2), 6.68–6.74 (3H, m, Ph-H); ^{13}C NMR (50 MHz, $CDCl_3$): δC (ppm) = 20.97 (CH_3), 34.36 (CH_2), 65.36 (CH_2), 115.24 (2 CH), 115.77 (CH), 130.19 (C), 142.64 (C), 143.99 (C), 171.69 (CO); MS (EI): *m*/*z* 340; elemental analysis: calcd C, 61.22; H, 6.16; O, 32.62, found C, 61.18; H, 6.15; O, 32.54.

5.5.7. Hydroxytyrosol propionate (4b)

Oil; ^{1}H NMR(400 MHz, $CDCl_3$): δH (ppm) = 1.08 (3H, m, CH_3), 2.28 (2H, m, CH_2), 2.78 (2H, m, CH_2), 4.20 (2H, m, OCH_2), 6.58–6.76 (3H, m, Ph-H); ^{13}C NMR (50 MHz, $CDCl_3$): δC (ppm) = 15.10 (CH_3), 27.45 (CH_2), 38.00 (CH_2), 65.95 (CH_2), 117.00 (2 CH), 124.10 (CH), 131.10 (C), 145.10 (C), 147.0 (C), 175.0 (CO); MS (EI): *m*/*z* 354; elemental analysis: calcd C, 62.85; H, 6.71; O, 30.44, found C, 62.81; H, 6.71; O, 30.49.

5.5.8. Hydroxytyrosol butyrate (4c)

Oil; ^{1}H NMR(400 MHz, $CDCl_3$): δH (ppm) = 0.88 (3H, m, CH_3), 1.58 (2H, m, CH_2), 2.25 (2H, m, CH_2), 2.78 (2H, m, CH_2), 4.21 (2H, m, OCH_2), 6.58–6.76 (3H, m, Ph-H); ^{13}C NMR (50 MHz, $CDCl_3$): δC (ppm) = 13.68 (CH_3), 18.72 (CH_2), 35.35 (CH_2), 36.82 (CH_2), 66.20 (CH_2), 116.98 (2 CH), 121.60 (CH), 130.30 (C), 144.24 (C), 144.45 (C), 173.22 (CO); MS (EI): *m*/*z* 368; elemental analysis: calcd C, 64.27; H, 7.19; O, 28.54, found C, 64.23; H, 7.19; O, 28.48.

5.5.9. Hydroxytyrosol pentanoate (4d)

Oil; ^{1}H NMR(400 MHz, $CDCl_3$): δH (ppm) = 0.95 (3H, m, CH_3), 1.64 (2H, m, CH_2), 2.24 (2H, m, CH_2), 2.75 (2H, m, CH_2), 4.24 (2H, m, OCH_2), 6.64–6.75 (3H, m, Ph-H); ^{13}C NMR (50 MHz, $CDCl_3$): δC (ppm) = 13.68 (CH_3), 18.72 (CH_2), 35.35 (CH_2), 36.82 (CH_2), 66.20 (CH_2), 116.14 (2 CH), 121.70 (CH), 130.30 (C), 144.45 (C), 174.22 (CO). MS (EI): *m*/*z* 382; elemental analysis: calcd C, 65.53; H, 7.61; O, 26.86, found C, 65.53; H, 7.69; O, 26.66.

6. Biological part

6.1. Viruses and cells

Poliovirus type 1 (Sabin strain) (VR-1562), Human echovirus type 9 (VR-1050), Herpes simplex type 1 (HSV-1: VR-260), Herpes simplex type 2 (HSV-2: VR-734) and Coxsackie type B3 (Cox B3: VR-1034), were propagated in African green monkey kidney cells (Vero: CCL-81). Adenovirus type 2 (VR-1080) and Adenovirus type 5 (VR-1523) were propagated in Human Epithelial type 2 cells (HEp2: CCL-23). Cytomegalovirus (CMV: VR-538) was propagated in Human Foreskin Fibroblast Cell (HFF-1: SCRC-1041). Viruses and cells were purchased from the American Type Culture Collection (ATCC). Cell lines were kept at 37 °C in a humidified atmosphere with 5% CO_2 and grown in Dulbecco's modified Eagle's Minimum Essential medium (DMEM) supplemented with 10% heat inactivated fetal calf serum (FCS), 2 mM L-glutamine, 0.1% sodium bicarbonate, 200 μg mL^{-1} of streptomycin and 200 units mL^{-1} of penicillin G. Working stocks of all viruses were prepared as cellular lysates using DMEM with 2% heat inactivated FCS (maintenance medium).

6.2. Biological assays

The compounds were initially dissolved in dimethyl sulfoxide (DMSO) and further diluted in maintenance medium before use to achieve the final concentration needed. The final dilution of test compounds contained a maximum concentration of 0.01% DMSO, which was not toxic to our cell lines. Acyclovir was used as the reference compounds.

6.3. Cell viability

The cytotoxicity of the test compounds was evaluated by measuring their effect on cell morphology and growth. Cell monolayers were prepared in 24-well tissue culture plates and exposed to various concentrations (μg/mL) of the compounds. Plates were checked by light microscopy after 24, 48, 72 and 96 h. Cytotoxicity was scored as morphological alterations (e.g., rounding up, shrinking, and detachment). Cell growth was determined by the 3-(4,5-dimethylthiazol-2-yl)-2,5-diphenyl tetrazolium bromide (MTT) method.[53] The cells were seeded at 1×10^4/mL (100 μL/well) in 96-well tissue culture plates such that cell replication remained logarithmic all along the 4-day incubation period. The 50% cytotoxic dose (CD_{50}) was expressed as the highest concentration of the compound that resulted in 50% inhibition of cell growth.

6.4. Antiviral activity

The assay of the antiviral activity against all the viruses tested was carried out by the 50% plaque reduction assay or by 50% virus-induced cytopathogenicity, as previously described.[54–56] The compound concentration required to inhibit virus plaque formation or virus-induced cytopathogenicity by 50% is expressed as the 50% effective concentration (ID_{50}) and calculated by dose–response curves and linear regression.

6.5. Effect of addition time

Monolayers of cells were grown to confluence in 24-well plates and inoculated with viruses at a MOI (multiplicity of infection) of 0.1. The plates were incubated for 2 h at 4 °C to ensure synchronous replication of the viruses, with or without compound R3 for the adsorption period. Then, the inoculum was removed and fresh medium, with or without the compound, was added at various times after the adsorption period. The plates were incubated at 37 °C for 12 h, then cultures were frozen and virus yield was determined by plaque assay.

6.6. Inhibition of virus adsorption

Infective center assay was used to study the effect of compound **3b** on the virus adsorption step. A VERO cell suspension (10^6 cells/mL) was cooled to 4 °C for at least 1h. HSV-1 (10^6 PFU/mL), incubated for 60 min at 37 °C with different concentrations of test compound, was cooled to 4 °C, and subsequently

added to the cell suspension. Cells were incubated with the virus-drug mixtures for 120 min at 4 °C to prevent the virus entering the cells. After the adsorption period, un-adsorbed virus and free compound were removed by washing three times with cold DMEM. The cells were then diluted serially and plaque assayed for cell-associated viral activity.

6.7. Cell culture pre-treatment

Pre-treatment of cultures was performed by exposing the cell monolayers to different concentrations of the test compound in maintenance medium for 1 and 2 days at 37 °C. After treatment the cell monolayers were washed thoroughly with PBS and infected with HSV-1 at a MOI of 0.1 to allow viral cytopathic activity. The cell monolayers grown in maintenance medium without the test compounds were used as control. Virus titration was performed as described above.

6.8. Virucidal activity

To test possible virucidal activity, equal volumes (0.5 mL) of viral suspension (containing 10^6 PFU/mL) and DMEM containing compound **3b** (5× the ID_{50}) were mixed and incubated for 1 h at 37 °C. Infectivity was determined by plaque assay after dilution of the virus below the inhibitory concentration.

Supplementary data

Supplementary data associated with this article can be found, in the online version, at http://dx.doi.org/10.1016/j.bmc.2015.07.061.

References and notes

1. Yum, S.; Doh, H. J.; Hong, S.; Jeong, S.; Kim, D. D.; Park, M.; Jung, Y. *Eur. J. Pharmacol.* **2013**, *699*, 124.
2. Coelho, V. R.; Vieira, C. G.; Pereira de Souza, L.; Moysés, F.; Basso, C.; Mausolff Papke, D.; Pires, T. R.; Siqueira, I. R.; Picada, J. N.; Pereira, P. *Life Sci.* **2015**, *122*, 65.
3. Zhang, L.; Ji, Y.; Kang, Z.; Li, C.; Jiang, W. *Toxicol. Appl. Pharmacol.* **2015**, *283*, 50.
4. Hsieh, M.-J.; Chien, S.-Y.; Chou, Y.-E.; Chen, C.-J.; Chen, J.; Chen, M.-K. *Phytomedicine* **2014**, *21*, 1746.
5. Ibrahim, A. S.; Sobh, M. A.; Eid, H. M.; Salem, A.; Elbelasi, H. H.; El-Naggar, M. H.; AbdelBar, F. M.; Sheashaa, H.; Sobh, M. A.; Badria, F. A. *Tumour Biol.: J. Int. Soc. Onco-developmental Biol. Med.* **2014**, *35*, 9941.
6. Lee, D.-H.; Kim, D.-W.; Jung, C.-H.; Lee, Y. J.; Park, D. *Toxicol. Appl. Pharmacol.* **2014**, *279*, 253.
7. Zinglé, C.; Tritsch, D.; Grosdemange-Billiard, C.; Rohmer, M. *Bioorg. Med. Chem.* **2014**, *22*, 3713.
8. Zhao, X.; Zhai, S.; An, M.-S.; Wang, Y.-H.; Yang, Y.-F.; Ge, H.-Q.; Liu, J.-H.; Pu, X. P. *PLoS One* **2013**, *10*, 78220.
9. Park, S. H.; Song, J. H.; Kim, T.; Shin, W. S.; Park, G. M.; Lee, S.; Kim, Y. J.; Choi, P.; Kim, H.; Kim, H. S.; Kwon, D. H.; Choi, H. J.; Ham, J. *Drugs* **2012**, *10*, 2222.
10. Pawar, R.; Das, T.; Mishra, S.; Nutan Pancholi, B.; Gupta, S. K.; Bhat, S. V. *Bio. Med. Chem. Lett.* **2014**, *24*, 302.
11. Gigante, B.; Santos, C.; Silva, A. M.; Curto, M. J. M.; Nascimento, M. S. J.; Pinto, E.; Pedro, M.; Cerqueira, F.; Pinto, M. M.; Duarte, M. P.; Laires, A.; Rueff, J.; Gonçalves, J.; Pegado, M. I.; Valdeira, M. L. *Biorg. Med. Chem.* **2003**, *11*, 1631.
12. Frey, K. M.; Gray, W. T.; Spasov, K. A.; Bollini, M.; Gallardo-Macias, R.; Jorgensen, W. L.; Anderson, K. S. *Chem. Bio. Drug Design* **2014**, *83*, 541.
13. Lee, C.; Lee, J. M.; Lee, N.-R.; Kim, D.-E.; Jeong, Y.-J.; Chong, Y. *Bio. Med. Chem. Lett.* **2009**, *19*, 4538.
14. Srinivasan, K. *Crit. Rev. Food Sci. Nutr.* **2014**, *54*, 352.
15. Kubra, I. R.; Rao, L. J. M. *Crit. Rev. Food Sci. Nutr.* **2012**, *52*, 651.
16. Saladino, R.; Gualandi, G.; Farina, A.; Nencioni, L.; Palamara, A. T. *Curr. Med. Chem.* **2008**, *15*, 1500.
17. Lemańska, K.; Van Der Woude, H.; Szymusiak, H.; Boersma, M. G.; Gliszczyńska-Swigło, A.; Rietjens, I. M. C. M.; Tyrakowska, B. *Free Rad. Res.* **2004**, *38*, 639.
18. Jeong, S.; Park, H.; Hong, S.; Yum, S.; Kim, W.; Jung, Y. *Eur. J. Pharm.* **2015**, *747*, 114.
19. Tabernero, M.; Sarriá, B.; Largo, C.; Martínez-López, S.; Madrona, A.; Espartero, J. L.; Bravo, L.; Mateos, R. *Food Func.* **2014**, *5*, 1556.
20. Sorensen, A. D. M.; Nielsen, N. S.; Yang, Z.; Xu, X.; Jacobsen, C. *Eur. J. Lipid Sci. Technol.* **2012**, *114*, 134.
21. Zhong, Y.; Shahidi, F. *J. Agric. Food Chem.* **2012**, *60*, 4.
22. Aparicio-Soto, M.; Sánchez-Fidalgo, S.; González-Benjumea, A.; Maya, I.; Fernández-Bolaños, J. G.; Alarcón-de-la-Lastra, C. *J. Agric. Food Chem.* **2015**, *63*, 838.
23. Georgiev, L.; Chochkova, M.; Totseva, I.; Seizova, K.; Marinova, E.; Ivanova, G.; Ninova, M.; Najdenski, H.; Milkova, T. *Med. Chem. Res.* **2013**, *22*, 4173.
24. Tofani, D.; Balducci, V.; Gasperi, T.; Incerpi, S.; Gambacorta, A. *J. Agric. Food Chem.* **2010**, *58*, 529.
25. Torres de Pinedo, A.; Penalver, P.; Pèrez-Victoria, I.; Rondòn, D.; Morales, J. C. *Food Chem.* **2007**, *105*, 657.
26. Bozzini, T.; Botta, G.; Delfino, M.; Onofri, S.; Saladino, R.; Amatore, D.; Sgarbanti, R.; Nencioni, L.; Palamara, A. T. *Bioorg. Med. Chem.* **2013**, *21*, 7699.
27. Ramsden, C. A.; Riley, P. A. *Bioorg. Med. Chem.* **2014**, *22*, 2388.
28. Ramey, A. M.; Reeves, A. B.; Sonsthagen, S. A.; Teslaa, J. L.; Nashold, S.; Donnelly, T.; Casler, B.; Hall, J. S. *Virology* **2015**, *482*, 79.
29. Palamara, A. T.; Brandi, G.; Rossi, L.; Millo, E.; Benatti, U.; Nencioni, L.; Iuvara, A.; Garaci, E.; Magnani, M. *Antiviral Chem. Chemother.* **2004**, *15*, 83.
30. Subrizi, F.; Crucianelli, M.; Grossi, V.; Passacantando, M.; Pesci, L.; Saladino, R. *ACS Catal.* **2014**, *4*, 810.
31. (a) Morgado, P. I.; Aguiar-Ricardo, A.; Correia, I. J. J. *Membrane Sci.* **2015**, *490*, 139; (b) Ariga, K.; Yamauchi, Y.; Rydzek, G.; Ji, Q.; Yonamine, Y.; Wu, K. C. W.; Hill, J. P. *Chem. Lett.* **2014**, *43*, 36; (c) Costa, R. R.; Mano, J. F. *Chem. Soc. Rev.* **2014**, *43*, 3453; (d) Decher, G.; Schmitt, J. *Prog. Colloid Polym. Sci.* **1992**, *89*, 160; (e) Decher, G. *Science* **1997**, *277*, 1232.
32. Shahi, A. Int. *Int. J. Pharm Biosc.* **2014**, *5*, 298.
33. Zhang, Q.; Huang, J.-Q.; Qian, W.; Zhang, Y.-Y.; Wei, F. *Small. Special Issue: Low-Dimensional Carbon Materials* **2013**, *9*, 1237.
34. Asuri, P.; Karajanagi, S. S.; Sellitto, E.; Kim, D.-Y.; Kane, R. S.; Dordick, J. S. *Biotechnol. Bioeng.* **2006**, *95*, 804.
35. Ziółkowska, D.; Shyichuk, A.; Zelazko, K. *Polimery* **2012**, *57*, 303.
36. Iamsamai, C.; Soottitantawat, A.; Ruktanonchai, U.; Hannongbua, S.; Dubas, S. T. *Carbon* **2011**, *49*, 2039–2045.
37. Robb, D. A.; Gutteridge, S. *Phytochemistry* **1981**, *20*, 1481.
38. Yua, C. M.; Yena, M.-J.; Chena, L. C. *Biosens. Bioelectron.* **2010**, *25*, 2515.
39. Piao, Y.; Jin, Z.; Lee, D.; Lee, H.-J.; Na, H.-B.; Hyeon, T.; Oh, M. K.; Kim, J.; Kim, H.-S. *Biosens. Bioelectron.* **2011**, *26*, 3192.
40. Migneault, I. *Biotecniques* **2004**, *37*, 790.
41. Liu, Y. J. *Membr. Sci.* **2011**, *132*, 385.
42. Masamoto, Y.; Iida, S.; Kubo, M. *Planta Med.* **1980**, *40*, 361.
43. Li, J.; Sha, Y. *Molecules* **2008**, *13*, 1111.
44. Mateos, R.; Trujillo, M.; Pereira-Caro, G.; Madrona, A.; Cert, A.; Espartero, S. L. *J. Agric. Food. Chem.* **2008**, *56*, 10960.
45. Lousa, D.; Baptista, A. M.; Soares, C. M. *Phys. Chem. Chem. Phys.* **2013**, *15*. 13723-1373.
46. James, S. H.; Larson, K. B.; Acosta, E. P.; Prichard, M. N. *Clin. Pharm., Therap.* **2015**, *97*, 66.
47. Manvar, D.; Pelliccia, S.; La Regina, G.; Famiglini, V.; Coluccia, A.; Ruggieri, A.; Anticoli, S.; Lee, J.-C.; Basu, A.; Cevik, O.; Nencioni, L.; Palamara, A. T.; Zamperini, C.; Botta, M.; Neyts, J.; Leyssen, P.; Kaushik-Basu, N.; Silvestri, R. *Eur. J. Med. Chem.* **2014**, *90*, 497.
48. Civitelli, L.; Panella, S.; Marcocci, M. E.; De Petris, A.; Garzoli, S.; Pepi, F.; Vavala, E.; Ragno, R.; Nencioni, L.; Palmara, A. T.; Angiolella, L. *Phytomedicine* **2014**, *21*, 857.
49. Saladino, R.; Neri, V.; Checconi, P.; Celestino, I.; Nencioni, L.; Palamara, A. T.; Crucianelli, M. *Chem. Eur. J.* **2013**, *19*, 2392.
50. Fioravanti, R.; Celestino, I.; Costi, R.; Cuzzucoli, G.; Crucitti, G.; Pescatori, L.; Mattiello, L.; Novellino, E.; Checconi, P.; Palamara, A. T.; Nencioni, L.; Di Santo, R. *Bioorg. Med. Chem.* **2012**, *20*, 5046.
51. Sgarbanti, R.; Nencioni, L.; Amatore, D.; Coluccio, P.; Fraternale, A.; Sale, P.; Mammola, C. L.; Carpino, G.; Gaudio, E.; Magnani, M.; Ciriolo, M. R.; Garaci, E.; Palamara, A. *Antioxid. Redox Signal.* **2011**, *15*, 593.
52. Palamara, A. T.; Nencioni, L.; Aquilano, K.; De Chiara, G.; Hernandez, L.; Cozzolino, F.; Ciriolo, M. R.; Garaci, E. J. *Infect. Dis.* **2005**, *191*, 1719.
53. Denizot, F.; Lang, R. *J. Imm. Methods* **1986**, *89*, 271.
54. Garozzo, A.; Cutrì, C.; Castro, A.; Tempera, G.; Guerrera, F.; Sarva, M. C.; Geremia, E. *Antivir. Res.* **2000**, *45*, 199.
55. Cutrí, C. C. C.; Garozzo, A.; Siracusa, M. A.; Sarvá, M. C.; Tempera, G.; Geremia, E.; Pinizzotto, M. R.; Guerrera, F. *Biorg. Med. Chem.* **1998**, *6*, 2271.
56. Haslam, E. *Shikimic Acid Metabolism and Metabolites*; John Wiley & Sons: New York, 1993.